

Electronic structures of and composition gaps among the ternary carbides Ti_2MC

G. Hug

Laboratoire d'Etudes des Microstructures, CNRS-ONERA, Boite Postale 72, 92322 Châtillon Cedex, France

(Received 13 January 2006; revised manuscript received 2 August 2006; published 13 November 2006)

The electronic structure of the Ti_2MC phases have been calculated in the framework of the full-potential augmented-plane-wave method under the general gradient approximation with $M=Al, Si, P, S, Sn, Ga, In, Ge, As, Pb,$ and Tl . Among these all but $M=Si, P, As$ give rise to stable compounds whose bonding is driven by $Ti d-M p$ and $Ti d-C p$ hybridizations. In general, $Ti d-M p$ hybridizations are located just below the Fermi level and are weaker bonds than the $Ti d-C p$ hybridizations, which are deeper in energy. As a function of the p -state filling of the M element the $Ti d-M p$ bands are driven to deeper energy. A transition occurs in the column of P and As whose p atomic energy levels match exactly the $C p$ ones. This explains why Ti_2PC and Ti_2AsC are not observed since P and As would link more favorably with C . Finally, the $Ti d-S p$ bonds are at lower energy and are stiffer than the $Ti d-C p$ bonds in the Ti_2SC compound. This shows that this compound must behave differently from the other Ti_2MC phases, as demonstrated by its elastic properties. In agreement with other previous studies, Ti_2SiC is found to be intrinsically stable but is not observed because it is in competition with other compounds in the $Ti-Si-C$ phase diagram.

DOI: 10.1103/PhysRevB.74.184113

PACS number(s): 62.20.Dc, 31.10.+z

I. INTRODUCTION

The ternary carbides consisting of one early transition metal T , one metal-like element M , and carbon form highly anisotropic structures of composition $T_{n+1}MX_n$ (here X denotes carbon or nitrogen since a few nitrides of the same composition and structure also exist). Such compounds were almost all synthesized in the 1960s by the group of Nowotny¹ in Vienna and are part of the so-called “Nowotny phases,” a wide class of ternary and quaternary carbides. Among them, those with $T_{n+1}MX_n$ formulas crystallize under an hexagonal crystal structure with a very large c/a ratio (Fig. 1). A large variety of compositions are available, mainly with $n=1$, in which case the phases are called also 211 for brevity. The prototype of the 211 phases is Cr_2AlC .^{3,2} Their properties were not considered for almost 30 years until they started to be synthesized systematically and characterized by Barsoum and El-Raghy.⁴ Indeed, these compounds exhibit several interesting properties, especially for use at high temperatures. Materials like Ti_3SiC_2 and Ti_2AlC are serious candidates for a number of practical applications at high temperature. Since the pioneering work of Barsoum and El-Raghy these materials are also referred as “MAX” phases but in this contribution the original “ T_2MX ” denomination is used.

Since 1998, the electronic structure of diverse compounds of this family has been studied by several groups⁵⁻¹¹ and is already well understood. In short, the bonding is achieved through a hybridization of T -atom d states with the M - and X -atom p states. A significant charge transfer of electrons towards the X atom is also observed, which contributes to the stability of the crystal. All these theoretical studies have been performed within density functional theory (DFT) and have been quite successful in predicting the stability and the elastic properties of this class of compound. Yet some of the physical properties have also been addressed directly *ab initio* allowing it to be understood how the anisotropy of the structure is responsible for the unusual properties. For

example, Yoo *et al.* have discovered that the Ti_3SiC_2 compound exhibits an almost negligible and constant thermopower over a very wide temperature range.¹² In the same way, recently, Chaput *et al.* have demonstrated that the thermopower tensor components have opposite contributions for the carriers in the basal plane and those along the hexagonal c axis.¹³ It therefore seems possible, for this class of materials, to predict, and maybe adjust, properties via *ab initio* calculations. One important step is to understand and predict the compositional stability domain of these phases.

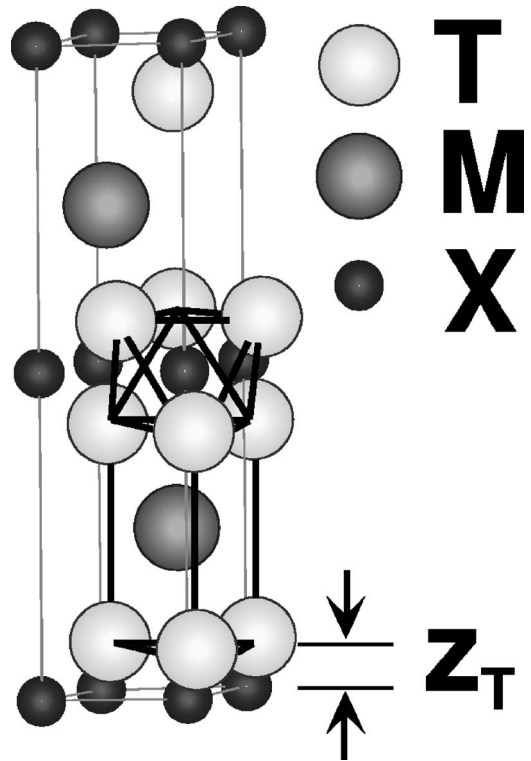


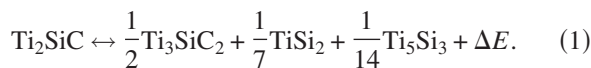
FIG. 1. Unit cell of the T_2MX phase. A $[T_6X]$ octahedron and a $[T_6M]$ trigonal prism are outlined.

TABLE I. The known 211 phases (after Jeitschko *et al.* (Ref. 2), Nowotny (Ref. 1) and Barsoum (Ref. 14). Each column corresponds to a column of the periodic table and $s^x p^y$ to the electronic configuration of the free M atom.

	$M s^2$	$M s^2 p^1$	$M s^2 p^2$	$M s^2 p^3$	$M s^2 p^4$
$T 3d$	Ti ₂ CdC	Sc ₂ InC Ti ₂ {Al, Ga, In, T}C V ₂ {Al, Ga}C Cr ₂ {Al, Ga}C Ti ₂ {Al, Ga, In}N V ₂ GaN Cr ₂ GaN	Ti ₂ {Ge, Sn, Pb}C V ₂ GeC Cr ₂ GeC	V ₂ {P, As}C	Ti ₂ SC
$T 4d$		Zr ₂ {In, Tl}C Nb ₂ {Al, Ga, In}C Mo ₂ GaC Zr ₂ {In, Tl}N	Zr ₂ {Sn, Pb}C Nb ₂ SnC	Nb ₂ {P, As}C	Zr ₂ SC Nb ₂ SC
$T 5d$		Hf ₂ {In, Tl}C Ta ₂ {Al, Ga}C	Hf ₂ {Sn, Pb}C Hf ₂ SnN		Hf ₂ SC

An interesting classification of the 211 compounds has recently been proposed by Sun *et al.*¹¹ These authors have shown that the 211 carbides based on transition metals of the VB and VIB groups retain the bulk modulus of their binary transition metal corresponding carbides. On the other hand, 211 phases based on the group IVB of transition metals exhibit a fairly large deviation from that of their corresponding binary carbide (see Fig. 1 of Ref. 11). They also pointed out that the valence of the M element does not affect the bulk modulus to the same extent as that of the transition metal, although they examined only two columns of the periodic table. Unfortunately, these results have not been confirmed in a recent publication.¹⁵ The authors point out that the choice of pseudopotential plays an important role in the elastic properties. Nevertheless, such work is important as it helps to understand the relationship between the properties and structure or composition and the stability domain of these phases. In the present paper, we use the full-potential method to study the influence of the M element in more detail. The full-potential method has an advantage over the pseudopotential, one of being, in principle, universal.

Due to their wide compositional spectrum, it is very exciting to try to optimize the properties of these compounds by alloying. In this respect, knowledge of the phase diagrams and especially the stability domain of different possible phases is very important for processing these materials or for trying to create new ones. For example, Palmquist *et al.*¹⁶ have studied the stability of the Ti₂SiC phase and they conclude that it could be stable with respect to decomposition to other phases of the ternary Ti-Si-C phase diagram following the reaction



Although very small, the $\Delta E = -8$ meV/atom corresponds to an equilibrium toward the left-hand side of this reaction in

contradiction of the fact that Ti₂SiC has never been synthesized experimentally. They further observed that the Ti₅Si₃ compound is likely to dissolve some C atoms in solid solution, which would further stabilize it, leading to the destabilization of the 211 phase. Therefore, the Ti₂SiC would not be stable, mainly because of neighboring competing phases.

In a different direction, Grechnev *et al.*¹⁷ have considered the possible existence of a hypothetical Nb₃SiC₂ compound.

All the 211 structures are summarized in Table I as a function of the electronic configuration of the M element rather than of the T metal.^{1,2,14} This presentation clearly reveals the effect of the p -band filling of the M element across the periodic table. The more numerous compounds are those in the aluminum column, and the occurrence of the 211 phases diminishes as the sp states are more and more filled. However, it is intriguing that Ti, Zr, and Hf atoms can bond to almost any M element from sp^2 to sp^4 , with the exception of the P, As column, but do form a compound with the S element. On the other hand, V and Nb, which are rather small atoms, can form compounds throughout the whole sp series.

The purpose of this contribution is to understand the physical origin of this composition gap in the {Ti, Zr, Hf}₂ MX series. The total energy of the Ti₂ MC phases is calculated utilizing the full-potential augmented-plane-wave (FP-APW) theory with a full optimization of the unit cell lattice and internal parameters.

In the next section (Sec. II), the numerical method which is used is briefly reviewed. Then, in Sec. III, the evolution of the bonding across the $s^2 p^x$ series will be presented and analyzed. In conclusion, a classification of the 211 phases is proposed.

II. THEORETICAL METHODS

The stability of a compound can be defined as an *absolute* or a *relative* stability. The absolute stability is an intrinsic

property and means that its free energy is an extremum with respect to small deformations and that extremum is a minimum. This has been addressed by calculating the total energy at 0 K *ab initio* within the density functional theory (DFT).¹⁸ This is not sufficient, however, for a compound to exist, since a competition with other phases in the phase diagram may also take place as in the case of the reaction in Eq. (1). This task is much more difficult to achieve from *ab initio* theory since it requires the calculation of several phases eventually off stoichiometry. Therefore, only a few calculations for strictly stoichiometric phases have been done for the specific case of Ti₂SiC.

The total energy and the electronic structure is calculated using the FP-APW method¹⁹ with a generalized gradient approximation²⁰ (GGA) within DFT as implemented in the now well-established WIEN2k code. The 211 phases have one free parameter, the z coordinate of the T atom (denoted z_T hereafter), in addition to the a - and c -lattice parameters. Therefore, an energy surface as a function of the volume of the unit cell and c/a ratio has been built, with approximately 25 points (5×5 matrix). For each point a minimization of the z_T parameter is achieved utilizing the reverse-communication trust-region quasi-Newton algorithm, which has been implemented by Marks²¹ in the WIEN2k code. A first fit with a two-dimensional quadratic function is made to check that the matrix is well centered around the absolute energy minimum; otherwise, more points are calculated. Then, for each volume, a fit of the energy as a function of c/a is achieved using a quadratic function. This procedure provides a set of points of energy E as function of the volume V for which both c/a and z_T are optimized. This set of data points is then fitted using the third-order Birch-Murnaghan equation^{22,23} of state to find the absolute energy minimum E_0 and volume V_0 and to derive the bulk modulus B_0 and its derivative B'_0 :

$$E(V) = E_0 + \frac{9V_0B_0}{16} \left\{ \left[\left(\frac{V_0}{V} \right)^{2/3} - 1 \right]^3 B'_0 + \left[\left(\frac{V_0}{V} \right)^{2/3} - 1 \right]^2 \times \left[6 - 4 \left(\frac{V_0}{V} \right)^{2/3} \right] \right\}. \quad (2)$$

Once the optimized volume is found it is used to determine the c/a and z_T parameters by interpolation. In order to analyze the elastic behavior of these compounds, the Ti-C and Ti- M interatomic distances and their derivative with respect to the pressure are calculated. The pressure is also derived from the Birch-Murnaghan model as follows:

$$P(V) = \frac{3B_0}{2} \left[\left(\frac{V_0}{V} \right)^{7/3} - \left(\frac{V_0}{V} \right)^{5/3} \right] \times \left\{ 1 + \frac{3}{4}(B'_0 - 4) \left[\left(\frac{V_0}{V} \right)^{2/3} - 1 \right] \right\}. \quad (3)$$

The formation energy has also been calculated as the difference between the total energy of the compound and the sum of the total energies of the elements involved. For this purpose the total energy of all the simple elements in their most stable form is calculated. However, to avoid a divergence in the number of calculations and because of the lack

of knowledge of all ternary phase diagrams, the total energy is compared to other binary or ternary compounds only for the specific case of Ti₂SiC.

III. RESULTS AND DISCUSSION

A. Crystal parameters and total energy

As a general remark, it must be emphasized that all the Ti₂MC phases, including the three hypothetical Ti₂SiC, Ti₂PC, and Ti₂AsC compounds, are intrinsically stable. Indeed, the plot of the energy surface with respect to the volume and c/a always presents a clear minimum. Thus, Ti₂SiC, Ti₂PC, and Ti₂AsC might be only metastable. The formation energies ΔE_f of the compounds are reported in Table II, as calculated from the difference between their total energies and the sum of the energies of the simple elements. They are always found to be negative, indicating that their formation is exothermic (however, with the noticeable exception of Ti₂PbC). Interestingly, this holds also for the three “unstable” compounds. In the case of Ti₂SiC, the energy balance of the equilibrium reaction [Eq. (1)] is also calculated. The ΔE found is small (-7.4 meV atom⁻¹) but in favor of the left-hand side of Eq. (1). This value is almost identical to the one previously determined by Palmquist *et al.*¹⁶ It confirms that Ti₂SiC should be stable or near the limit of stability. In the case of Ti₂PbC the total energy calculation has been performed with or without spin orbit coupling (SOC) in order to take into account relativistic corrections. In both cases ΔE_f is found to be unfavorable for the formation of the compound. The introduction of the SOC improves slightly the situation, and it therefore this value which is reported in Table II. Since Ti₂PbC does exist, the calculation fails in this case for reasons which are not presently fully clarified but the results concerning this compounds should be considered with care.

The optimized crystallographic parameters (a , c , and z_T) are reported in Table II. They are in good or very good agreement with the already published lattice parameters (see Barsoum¹⁴). Since both lattice parameters and the internal relaxation parameter (z_T) result from the energy minimization procedure, it is easy to calculate all necessary geometrical crystallographic parameters. Of interest are the crystal units that can be considered as the building blocks to describe the compound. In the 211 phases these blocks are the $[T_6X]$ octahedra and the $[T_6M]$ triangular prisms (Fig. 1). The octahedra have a cubic point symmetry $m\bar{3}m$, with fourfold and threefold axes, and the trigonal prism triangular symmetry $\bar{6}/m2$ only. The association of these two polyhedra leads to the $P6_3/mmc$ hexagonal space group, when building an infinite crystal, although in such a case the octahedron loses its fourfold axis and a relaxation is observed while its point symmetry is lowered to $\bar{3}m$. Previously, we have defined a parameter a_r which measures the amount of “noncubic” distortion of the octahedron.²⁴ It can be defined as

$$a_r = \frac{\sqrt{3}}{2 \sqrt{4z_T^2 \left(\frac{c}{a} \right)^2 + \frac{1}{12}}}. \quad (4)$$

The factor a_r equals unity for the cubic octahedron. Similarly, it is possible to define an ideal trigonal prism corre-

TABLE II. Results of the FP-APW calculations for the known Ti_2MC compounds and below the separation line for the hypothetical compounds. The equilibrium lattice parameters a and c are compared to experimental ones. The relaxed atomic coordinates z_T are also given. The bulk moduli (B_0), the TDOS at Fermi energy, and the formation energy (ΔE_f) are also shown.

	a (pm)	a_{expt} (pm)	c (pm)	c_{expt} (pm)	z_T	B_0 (GPa)	DOS at E_F (state/eV/uc)	ΔE_f (eV atom $^{-1}$)
Ti_2AlC	307.0	304	1376.8	1360	0.0833	137	2.67	-0.71
Ti_2GaC	308.1	307	1346.8	1352	0.0848	129	2.55	-0.93
Ti_2InC	314.4	313	1424.6	1406	0.0778	121	2.39	-1.2
Ti_2TlC	317.7	315	1425.5	1398	0.0771	139	2.35	-0.82
Ti_2GeC	309.0	307	1304.0	1293	0.0885	163	3.83	-0.99
Ti_2SnC	317.1	316.3	1385.7	1367.9	0.0807	167	3.71	-2.32
Ti_2PbC	323.9	320	1413.4	1381	0.0765	140	4.73	2.4
Ti_2SC	318.6	321.6	1123.1	1122	0.0993	176	1.55	-1.55
Ti_2SiC	305.2		1287.3		0.0916	167	3.17	-0.86
Ti_2PC	319.1		1145.7		0.1019	163	5.99	-1.02
Ti_2AsC	320.9		1192.5		0.0943	175	5.25	-0.82

sponding to a packing of hard spheres of equal diameter and a distortion parameter p_r :

$$p_r = \frac{1}{\sqrt{\frac{1}{3} + \left(\frac{1}{4} - z_T\right)^2 \frac{c^2}{a^2}}}. \quad (5)$$

p_r is also equal to 1 for the ideal prism.

These two parameters a_r and p_r are reported in Table II and displayed in Fig. 2. It is obvious from the figure that the effect of increasing the valence of the M atom is to distort both polyhedral structural units, although the prism is much more affected.

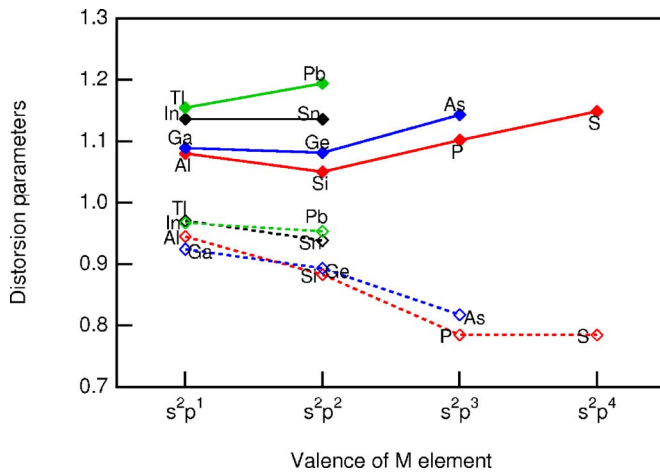


FIG. 2. (Color online) Evolution of the distortion parameters of the octahedral [a_r , Eq. (4), solid symbols and solid lines] and prismatic [p_r , Eq. (5), open symbols and dashed lines] crystal units as a function of the M p -shell filling. Colors correspond to the different shells: red, 3 p ; blue, 4 p ; black, 5 p ; and green, 6 p .

B. Density of states

The values of the total density of states (TDOS) at the Fermi level (E_F) are reported in Table II and in Fig. 3. They are for most of them below 4 states eV^{-1} . As a general trend, it is observed that the TDOS at E_F increases with the p -state filling of the M element. It presents a maximum for Ti_2PC and Ti_2AsC with values above 5 states eV^{-1} , followed by a sharp decrease for Ti_2SC . Thus Fig. 3 shows nicely the general trend that the metallicity of the compound increases with the filling of the p states of the M element and that a sharp transition to a more ceramiclike behavior occurs in the column of S.

Figure 4 shows that the TDOS around the Fermi level (E_F) generally lies in a dip. This location is consistent with a separation position between the bonding and antibonding states. However, the TDOS of the compounds with the s^2p^3 M atoms presents a sharp peak at E_F , a configuration which

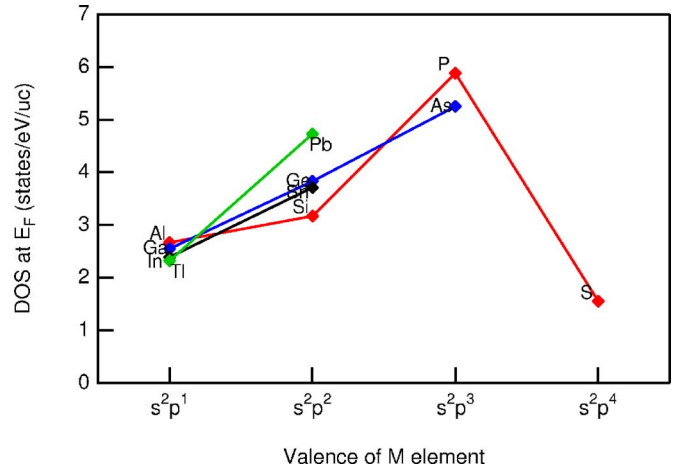


FIG. 3. (Color online) Values of the TDOS at Fermi level as a function of the p -shell filling. Same color code as in Fig. 2.

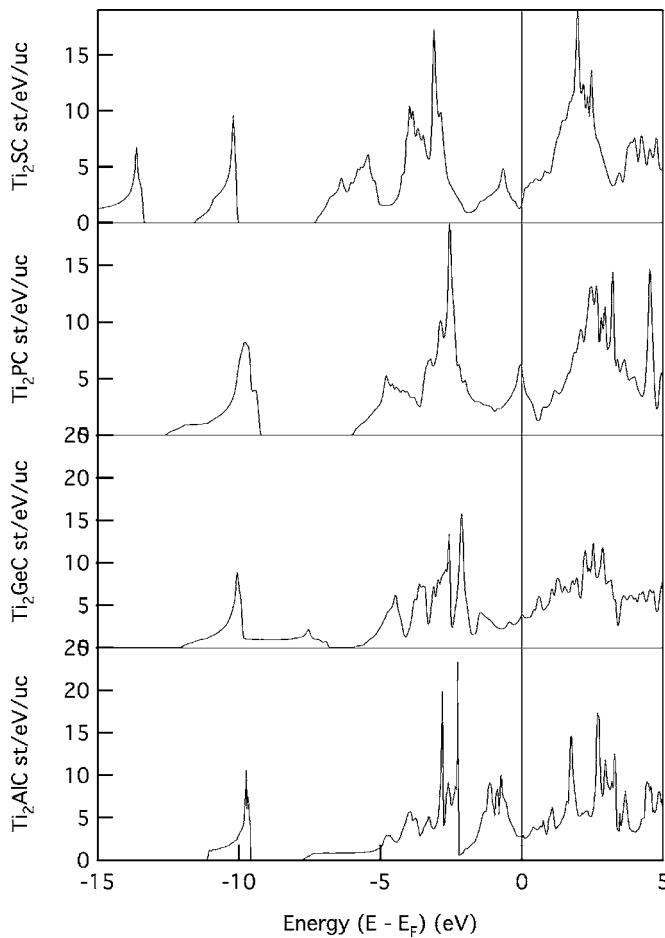


FIG. 4. TDOS for selected compounds from the different columns of the periodic table. From bottom to top: Ti_2AlC , Ti_2GeC , Ti_2PC , and Ti_2SC .

is often associated with a structural instability.

More understanding can be gained by examination of the partial DOS which are displayed for selected compounds in Fig. 5. All the compounds share the same bonding scheme consisting of Ti d -C p and Ti d -M p hybrids as has been widely discussed in the literature. In the majority of $T_{n+1}MX_n$ phases, the bonds between the transition metal and carbon are strong and found to lie at a lower energy than the T -M bonds. Indeed, for the compounds whose M electronic configuration is s^2p^1 or s^2p^2 , E_F is found to be located in a dip above a Ti d -M p hybrid and below the broad Ti d unfilled band. As is known, the p states of the M atom are shifted to lower energy as the filling of the p band is increased. Therefore, the Ti d -M p hybrids are located at increasingly lower energy when the M atom is shifted towards the right side of the periodic table. From the present calculations, for the most filled M p band (Ti_2SC) the S p states are found at lower energy than the C p states, suggesting that an inversion in the strength of the two kinds of bonds occurs.

In the case of P or As, the calculation shows that the two hybrids Ti d -P p and Ti d -As p are located exactly at the same energy as the Ti d -C p hybrid. Thus, that column of the periodic table clearly marks a separation between two different regimes. In order to build a first charge density to

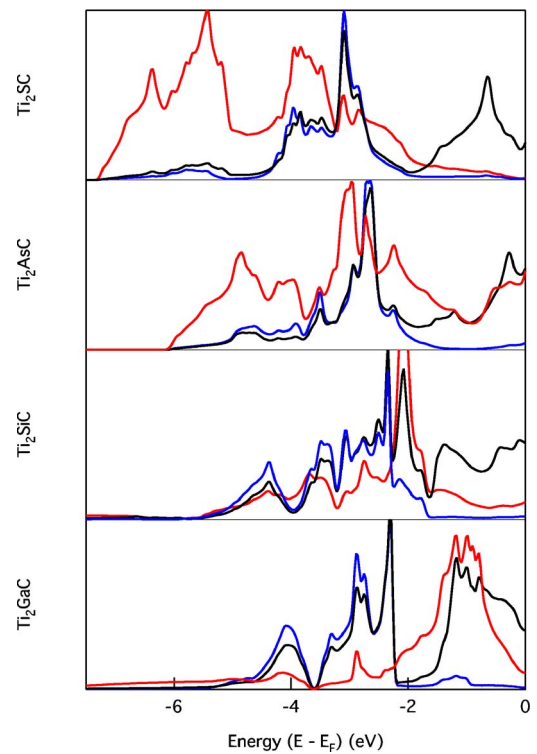


FIG. 5. (Color online) Partial DOS showing the Ti d -C p and the Ti d -M p hybridizations for selected compounds. The Ti d , C p , and M p states are black, blue, and red, respectively. The Ti d -M p hybridization is shifted to lower energy as the M p shell becomes more filled. Note that for clarity the relative intensities of the partial DOS are not preserved. From bottom to top: Ti_2GaC , Ti_2SnC , Ti_2AsC , and Ti_2SC .

start the self-consistent minimization, the WIEN2k code uses the Desclaux algorithm to calculate an atomic charge density of the free atoms. From that step, the atomic energy levels can be extracted and it is found that the atomic p levels of C, P, and As are almost at the same energy whereas the Ti d levels are slightly above. This could suggest that the C and P (or As) atoms are more likely to share electrons together rather than with Ti in which case they would need to gain energy.

Since it is not experimentally observed, the case of Ti_2SiC needs also to be examined in some detail. It can be seen that this compound bears the same features as the other stable 211 phases of the family. It has a relatively low DOS at E_F , which is located at a dip, and the two kinds of hybrids are clearly separated in energy. This confirms the intrinsic stability of this phase as proposed by Palmquist *et al.*¹⁶ and by the present full-potential calculation.

C. Elastic properties

The increase of p electrons from M atoms when moving rightwards along the periodic table results in an increase of the bulk moduli up to the s^2p^3 column as can be seen in Fig. 6. This behavior is expected since the shift of the Ti d -M p hybrid to lower energy and its higher filling is obviously expected to lead to stronger bonds. Since these phases con-

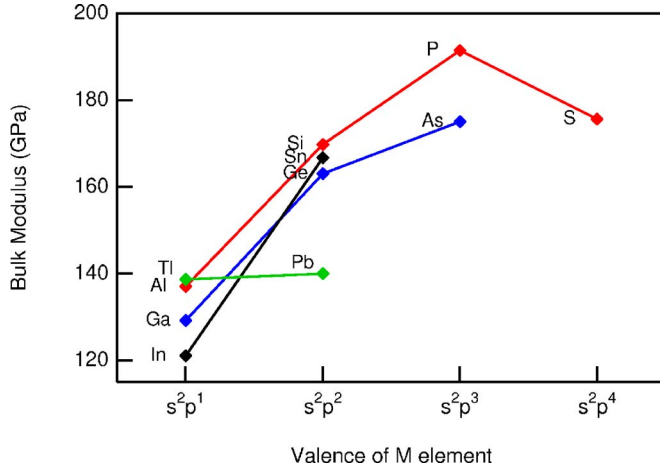


FIG. 6. (Color online) Bulk moduli of the compounds as a function of the M p -shell filling. Same color code as in Fig. 2.

sist of a mixture of “soft” T - M and “hard” T - X ” bonds, it is reasonable that the strengthening of the softer bond results in an increase of the bulk modulus. The crystalline structure may be viewed as an alternation of soft and hard bonds along the c axis which can therefore be considered as springs in series and therefore, in that direction, the elastic behavior is controlled by the soft bond. A saturation seems to occur after the column of the s^2p^3 elements, i.e., for Ti_2SC , whose bulk modulus is somewhat lower than those of Ti_2PC and Ti_2AsC .

A similar increase of the bulk modulus with p electron concentration at the M site was also recently reported in the case of Zr_2MC and Ta_2MC family.²⁵

More insight can be gained by looking at the way the bond lengths evolve with pressure. The total energy as a function of volume has been fitted to the third-order Birch-Murnaghan equation of state,^{22,23} out of which the pressure has been extracted [Eqs. (2) and (3)]. Then, the interatomic distances between Ti and C atoms and between Ti and M atoms are recalculated from the optimized crystallographic parameters a , c , and z_T as a function of pressure. The bond lengths as a function of pressure are fitted by a straight line whose slope defines the bond stiffnesses k_{TM} and k_{TX} for T - M and T - X , respectively. These results are reported in Table III and plotted in Fig. 7. It can be seen that k_{TM} decreases across the periodic table whereas k_{TX} is relatively constant. This is in agreement with the expected behavior and the literature concerning these phases. It is remarkable to note that, in the case of the hypothetical “unstable” compounds Ti_2PC and Ti_2AsC , the stiffness is almost identical for both kinds of bond, which has to be related to the same energy position of the two hybrids as shown by the analysis of the DOS discussed earlier (Sec. III B). Such a behavior seems to characterize these compounds which are not easy to synthesize. Yet, for Ti_2SC , the stiffness is still different for the two kinds of bonds. The Ti-S bond stiffness is lower than for the Ti-C bond, a fact which can be correlated with the filling of anti-bonding orbitals as the p states of S are almost totally filled.

The s^2p^3 column of the periodic table seems to mark a limit between two regimes where elastic properties are different. It correspond to correlated positions of a maximum of

TABLE III. Interatomic distances and their derivatives as a function of pressure for the Ti_2MC compounds.

	d_{TM} (pm)	d_{TX} (pm)	k_{TM} (pm GPa ⁻¹)	k_{TX} (pm GPa ⁻¹)	a_r	p_r
Ti_2AlC	289.8	211.1	-1.37	-0.438	1.080	0.945
Ti_2GaC	285.0	211.4	-1.09	-0.319	1.089	0.925
Ti_2InC	305.1	212.3	-1.81	-0.568	1.136	0.971
Ti_2TiC	307.2	213.9	-1.97	-0.594	1.155	0.967
Ti_2GeC	275.7	212.4	-1.10	-0.502	1.081	0.893
Ti_2SnC	297.5	214.6	-1.35	-0.511	1.136	0.938
Ti_2PbC	308.7	215.8	-1.15	-0.331	1.180	0.950
Ti_2SC	251.4	216.1	-0.619	-0.379	1.148	0.785
Ti_2SiC	269.4	211.9	-0.820	-0.383	1.050	0.883
Ti_2PC	250.5	218.1	-0.466	-0.477	1.101	0.785
Ti_2AsC	262.3	216.7	-0.628	-0.631	1.143	0.817

DOS at Fermi energy and a maximum of the bulk modulus. As in the case of elastic properties; one could expect that other properties (electronic, optical, etc.) from phases on both sides of this limit are also different.

IV. CONCLUSIONS

The theoretical values of the lattice parameters and the crystallographic free parameter z_T of the Ti_2MC phases are reported for a large number of M elements in order to infer general tendencies. The z_T parameter has not yet been experimentally determined for most of them, and the present results should be useful for future work on these phases. As already known, the origin of the stability of the Ti_2MC phases is related to Ti d - M p and Ti d - C p bonds. For the M elements with the lowest filled p states, the Ti d - C p bonds are lower in energy and stiffer than the Ti d - M p bonds. A transition occurs at the {P, As} column of the periodic table,

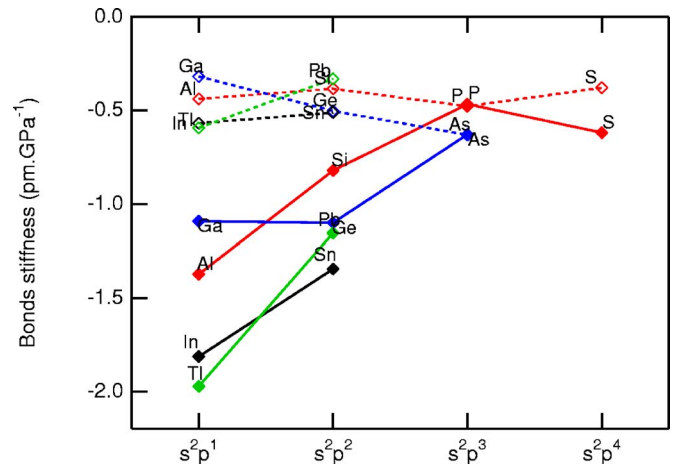


FIG. 7. (Color online) Relative stiffness of the T - M (solid symbols and solid lines) and T - X (open symbols and dashed lines) bonds as a function of the M p -shell filling. Same color code as in Fig. 2.

for which the p atomic levels of C and P/As are almost exactly at the same energy whereas the Ti d atomic levels are slightly above them. In this case, the C {P, As} elements are more likely to bond together rather than with Ti, leading to a composition gap in the p series of the Ti-based phases. This leads probably to a metastable state only since all other intrinsic parameters suggest that the structure is stable. For the phases with higher p -state filling like S, the $M p$ states are lower in energy than the $C p$ states. As a consequence, the Ti d -S p hybrid is lower in energy than the Ti d -C p . This inversion of the energy hierarchy leads to the shortest and stiffest Ti- M bonds for all Ti_2MC phases. These considerations also explain the trends in the c/a ratio for these phases. In addition, the TDOS at the Fermi level is higher for

the unstable structures (Ti_2PC , Ti_2AsC) whereas the Fermi level of the stable structures is located at or close to a minimum in the TDOS. In conclusion, it is proposed to classify the 211 structure into two categories, depending upon the hierarchy in energy of the Ti d - $M p$ and Ti d - $X p$ hybrids. It can be postulated that these two types may exhibit different properties.

ACKNOWLEDGMENTS

The author is grateful to Michel Jaouen (Poitiers University) and Denis Gratias (LEM, CNRS-ONERA) for stimulating discussions and suggestions.

-
- ¹H. Nowotny, Prog. Solid State Chem. **2**, 27 (1970).
²W. Jeitschko, H. Nowotny, and F. Benesovsky, J. Less-Common Met. **7**, 133 (1964).
³W. Jeitschko, H. Nowotny, and F. Benesovsky, Monatsch. Chem. **94**, 672 (1963).
⁴M. W. Barsoum and T. El-Raghy, J. Am. Ceram. Soc. **79**, 1953 (1996).
⁵N. I. Medvedeva, D. L. Novikov, A. L. Ivanovsky, M. V. Kuznetsov, and A. J. Freeman, Phys. Rev. B **58**, 16042 (1998).
⁶S. F. Matar, Y. L. Petitcorps, and J. Etourneau, J. Mater. Chem. **7**, 99 (1997).
⁷G. Hug and E. Fries, Phys. Rev. B **65**, 113104 (2002).
⁸J. M. Schneider, Z. Sun, R. Mertens, F. Uestel, and R. Ahuja, Solid State Commun. **130**, 445 (2004).
⁹Z. Sun, R. Ahuja, and J. M. Schneider, Phys. Rev. B **68**, 224112 (2003).
¹⁰Z. Sun, R. Ahuja, S. Li, and J. M. Schneider, Appl. Phys. Lett. **83**, 889 (2003).
¹¹Z. Sun, D. Music, R. Ahuja, S. Li, and J. M. Schneider, Phys. Rev. B **70**, 092102 (2004).
¹²H.-I. Yoo, M. W. Barsoum, and T. El-Raghy, Nature (London) **407**, 581 (2000).
¹³L. Chaput, G. Hug, P. Pécheur, and H. Scherrer, Phys. Rev. B **71**, 121104(R) (2005).
¹⁴M. Barsoum, Prog. Solid State Chem. **28**, 201 (2000).
¹⁵D. Music, Z. Sun, R. Ahuja, and J. M. Schneider, Phys. Rev. B **73**, 134117 (2006).
¹⁶J.-P. Palmquist *et al.*, Phys. Rev. B **70**, 165401 (2004).
¹⁷A. Grechnev, S. Li, R. Ahuja, O. Eriksson, U. Jansson, and O. Wilhelmsson, Appl. Phys. Lett. **85**, 3071 (2004).
¹⁸W. Kohn and L. J. Sham, Phys. Rev. **140**, A1133 (1965).
¹⁹P. Blaha, K. Schwarz, P. Sorantin, and S. Trickey, Comput. Phys. Commun. **59**, 399 (1990).
²⁰J. P. Perdew, K. Burke, and M. Ernzerhof, Phys. Rev. Lett. **77**, 3865 (1996).
²¹P. Blaha, K. Schwarz, G. K. H. Madsen, D. Kvasnicka, and J. Luitz, WIEN2k An Augmented Plane Wave+Local Orbitals Program for Calculating Crystal Properties, Karlheinz Schwarz, Technical Universität Wien, Austria, 2001.
²²F. Birch, Phys. Rev. **71**, 809 (1947).
²³F. Birch, J. Geophys. Res. **86**, 1257 (1978).
²⁴G. Hug, M. Jaouen, and M. W. Barsoum, Phys. Rev. B **71**, 024105 (2005).
²⁵J. M. Schneider, D. Music, and Z. Sun, J. Appl. Phys. **97**, 66105 (2005).